Numerical simulation of noise generated by multi asperity contact between rough surfaces

Viet Hung Dang, Alain Le Bot, Joël Perret Liaudet

ACOUSTICS 2012

Numerical simulation of noise generated by multi asperity contact between rough surfaces

V.H. Dang, A. Le Bot and J. Perret Liaudet

Laboratoire de Tribologie et Dynamique des Systèmes, 36 Avenue Guy de Collongue, 69134 Ecully Cedex
viet-hung.dang2@ec-lyon.fr

The friction between heterogeneous, rough and complex surfaces induces vibration in the solids and radiates noise in the surrounding media. In this study, we propose a numerical approach based on a modal development to estimate the statistical properties of local dynamics which cannot be obtained by experiments. The approach consists in three algorithms : the contact detection, the calculation of contact forces and the time integration of the governing equations. The validation of the method is then discussed by comparison with the finite element software Abaqus and some experimental results. The calculation results show that noise is an increasing function of the surface roughness and sliding speed. The basic mechanism responsible of noise is asperity shocks occurring at the interface that convert a part of the kinetic energy of the sliding solid into acoustical energy.

1 Introduction

When two objects are rubbed against each other, they generate friction noise. These noises occur very often in everyday life such as: door hinges, rail-wheel noise, brake noise,... From the physical point of view, they can be divided into at least two major groups according to the contact pressures. When the contact pressure is high, the friction noise stems from mechanical instabilities such as sprag-slip, stick-slip. On the other hand, when the contact pressure is low, the friction noise is called roughness noise. Moving a small object on a table or rubbing the hands against each other are two examples of roughness noise. This is a direct effect of the dynamics rough interfaces. Firstly, the interaction of rough surfaces during the relative movement generates many shocks of opposite asperities. Secondly, the whole structure loaded by interaction forces, vibrates on its own eigenmodes. Finally, the sound is radiated from structure to environment. In this paper, we

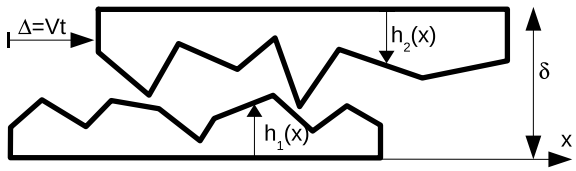

Figure 1: *Shift of two rough profiles. Elevations h_i are counted so opposite. The gap between the two profiles is δ. At time t, the horizontal offset is imposed $\Delta = Vt$*

present a numerical approach to study the noise induced by the contact between two rough surfaces. The model is made up of two rough profiles interacting plane-plane as in Fig. 2. The high profile moves horizontally with constant velocity V, while the lower one is fixed at both ends. The initial gap between the two profiles is δ. We note that there is a combination of an initial-boundary-value problem and a contact problem. So that, we use the algorithms of boundary element methods to compute the contact force and the time integration schemes to solve numerically the governing equation of motion at each time increment. For this model, we can use these assumptions :

- Euler-Bernoulli beams.
- The horizontal position of nodes is imposed (no longitudinal vibration).
- Signorini's condition of non-penetration at the interfaces.

2 Governing equation of motion

The governing equation for the transverse motion of a beam :

$$D_i\Delta^2 u_i + m_i\frac{\partial^2 u_i}{\partial t^2} = f(t,x), \tag{1}$$

where u_i is the deformation of beam and f the contact force field applied to the beam. $D = EI$ is bending stiffness, E_i Young's modulus and I_i the moment of inertia, m_i is the mass per unit length. For a pinned-pinned beam, the boundary conditions are :

$$u_i(0) = u_i''(0) = u_i(L_i) = u_i''(L_i) = 0. \tag{2}$$

The eigenmodes ψ_i^k with $k = 0, 1, ...$ of beam i are defined so that,

$$\int_0^{L_i} \psi_i^k(x)\psi_i^l(x)dx = \delta^{kl} \tag{3}$$

$$D_i\Delta^2\psi_i^k = m_i(\omega_i^k)^2\psi_i^k \tag{4}$$

They are given by : $\psi_i^k(x) = \sqrt{\frac{2}{L_i}}\sin(k+1)\frac{\pi x}{L_i}$ and $\omega_i^k = \sqrt{\frac{D_i}{m_i}}\left(\frac{(k+1)\pi}{L_i}\right)^2$ The displacement u_i can be written as a sum of modal contribution of the form

$$u_i(t,x) = \sum_{k=0}^{\infty} U_i^k(t)\psi_i^k(x) \tag{5}$$

By using orthogonality of eigenmodes, it yields

$$m_i\left[\ddot{U}_i^k + (\omega_i^k)^2 U_i^k\right] = F_i^k(t) \tag{6}$$

with the modal force F_i^k defined by $F_i^k(t) = \int_0^{L_i} f(t,x)\psi_i^k(x)dx$. In the case of a damped structure, we rather have

$$m_i\left[\ddot{U}_i^k + 2\zeta_i^k\omega_i^k\dot{U}_i^k + (\omega_i^k)^2 U_i^k\right] = F_i^k(t) \tag{7}$$

This differential equation can be written as a first order ordinary differential equation :

$$\begin{bmatrix} \dot{U}_i^k \\ \dot{V}_i^k \end{bmatrix} = \begin{bmatrix} 0 & 1 \\ -\left(\omega_i^k\right)^2 & -2\omega_i^k\zeta_i^k \end{bmatrix}\begin{bmatrix} U_i^k \\ V_i^k \end{bmatrix} + \begin{bmatrix} 0 \\ F_i^k \end{bmatrix} \tag{8}$$

By introducing $y = \begin{bmatrix} U(t) \\ V(t) \end{bmatrix}$ we obtain the standard form of an initial value problem (IVP problem) :

$$\dot{y} = g(y)\ ;\ y(0) = 0 \tag{9}$$

For solving numerically a structural dynamics problem, the space-time discretization is mostly used. The time interval [0,T] is divided into equal subintervals of time step τ. The surface is discretized into element with the surface interval χ_i. We set $t^m = m\tau$, $x_i^n = n\chi_i$ and the modal values $U_i^{m,k} = U_i^k(t^m)$ et $\psi_i^{k,n} = \psi_i^k(x_i^n)$.

3 Contact algorithm

We consider one point $x_1$on the higher surface. The vertical distance between this point with the lower surface is given by

$$g(t,x) = h_1(x) + u_1(t,x) + h_2(x-\Delta) + u_2(t,x-\Delta) - \delta \quad (10)$$

We denote f the contact pressure at x_1 then the condition non-penetration, also called Signorini condition is :

$$g \geq 0\ ;\ f \leq 0\ ;\ g.f = 0 \quad (11)$$

In this study, we use two methods to computer the contact force : the penalty and the multiplier Lagrange. Firstly, with the penalty, we accept a low penetration between two solids, then the contact force is computer by a linear relation $f(t,x) = \kappa e(t,x)$. Here, κ is the penalty parameter. Its value is empirically chosen. A too low penalty parameter lead to a high penetration, otherwise a very high value will cause an ill-conditioned numerical problem.
The second method, multiplier Lagrange method, the non-penetration condition is fully respected , $g \geq 0$, In each increment of the analysis, the kinematic state of the model is first computed without considering the contact, then the penetrations are determined. The next step, we resolve a system equation to determine multiplier Lagrange (contact force) and acceleration corrections. These acceleration corrections are used to obtain a corrected configuration in which the contact constraints are enforced.

4 Time integration scheme

In this section, we present six time integration schemas in order to approximate numerically solutions of IVP. Thus, we can obtain value of displacement, contact force, vibratory velocity at each point and each time increment. The evaluation of a scheme is based on three criteria: consistency, stability and convergence. The scheme is consistent if the maximum of the error at each time increment tends to 0 when the time step becomes small. The scheme is stable, if the propagation of rounding errors can be controlled over the calculations. A scheme consistent and stable is said to be convergent meaning that the global error (difference between exact solution and scheme solution) tends to 0 when the step becomes small. Tab. **??** summarizes the character schemes used. Thanks to the consistency, stability and ease of implementation, we chose the backward Euler as the main scheme to perform calculations.

5 Validation

We present two numerical tests to validate accuracy of the proposed approach. In the first example, a simple and representative model formed by two simple rough surfaces rubbed together is used to compare our programs ra2D with the finite element software ABAQUS. The upper surface consist of only one peak, whereas the lower consisting of 6 peaks. The mesh topology, boundary conditions and material properties are shown in Fig. 2. We employed a mesh with 2874 nodes, 850 CPE6 (6-node triangular plane strain) elements.
Fig. 3 shows a comparison of displacement and pressure

Method	Time step	Local error	Property
Midpoint	$\tau < \frac{2}{\omega_i^k}$	$o\left(\tau^2\right)$	Explicit multiple step
Euler ex.	instable	$o\left(\tau\right)$	Explicit one step
Euler backward		$o\left(\tau^2\right)$	Implicit one step
RK2 -Heun	$\tau < \frac{\sqrt{2}}{\omega_i^k}$	$o\left(\tau^2\right)$	Explicit one step
RK4		$o\left(\tau^4\right)$	Explicit one step
RK8		$o\left(\tau^5\right)$	Explicit one step

Table 1: Time integration scheme

contact at the summit of peak on the upper surface. The obtained results present a good agreement between two programs. There are although some differences, mostly in amplitude of contact pressure. The main reason is that only modes vibration in audible band of solid are remained, thus the local deformation is not totally simulated. In the term of CPU time, it takes 280s with Abaqus and only 30s with Ra2D. Ra2D is around ten times faster. In the second test,

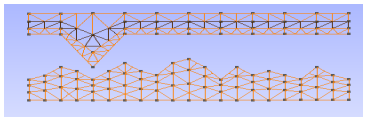

Figure 2: Mesh of the test case sixChocs

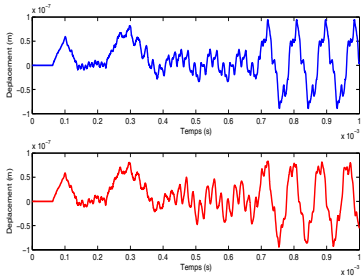

(a) Displacement of asperity on upper solid

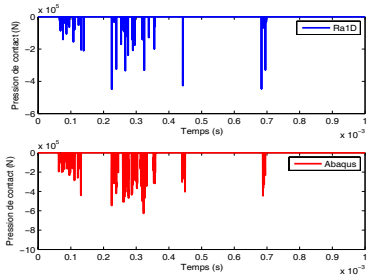

(b) Contact pressure of asperity on upper solid

Figure 3: Comparaison of numerical results between ra2D and Abaqus

we compare ra2D with an analytical solution of moving load problem. A simple supported beam subjected to a

moving mass at a constant speed. The analytical solution is presented in Olsson [5]. In Fig. 4, we plot the deflection of the middle of the beam over time with different speeds of the moving mass. Perfect agreement between the results obtained by ra2D with the analytical solution, is observed.

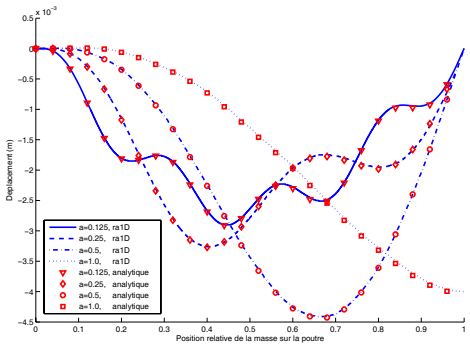

(a) Displacement at middle point of beam

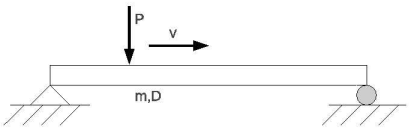

$$u(x,t) = \frac{2PL^3}{\pi^4 D}\sum_{n=1,\alpha\neq n}^{\infty}\left[\frac{1}{n^2(n^2-\alpha^2)}\left(\sin\left(\frac{n\pi tv}{L}\right)-\frac{\alpha}{n}\sin\left(\frac{n^2\pi tv}{\alpha L}\right)\right)\sin\left(\frac{n\pi x}{L}\right)\right]$$
$$+\frac{2PL^3}{\pi^4 D}\left[\frac{1}{2\alpha^4}\left(\sin\left(\frac{\alpha\pi tv}{L}\right)-\frac{\alpha\pi tv}{L}\cos\left(\frac{\alpha\pi tv}{L}\right)\right)\sin\left(\frac{\alpha\pi x}{L}\right)\right]$$

(b) Moving load on a beam

Figure 4: Comparaison ra2D / solution analytique pour une masse mobile sur poutre

6 Simulation results

Two solid with rough surfaces are randomly generated with a gaussian height distribution. The imposed parameters are Rq : the root mean square height, Rsm : asperities spacing, number of surface points, and length of surface. The dimensions are 300x200x2mm for the resonator and 20x20x20mm for the slider. They are made of steel with a Young's modulus $E = 210GPa$, a Poisson's coefficient $\nu = 0,3$, a volumic mass $\rho = 7800kg/m^3$ and a structural damping of 0,02. The data required for the simulation time step $\tau = 1e^{-8}s$, space step $\chi = 8\mu$m and duration of simulation $T = 1s$. The first result is that the CPU time

Rq (μm)	Rt (μm)	Rz (μm)	Ra (μm)	Rku	RSm (μm)
02	12.8	6.0	1.7	3.6	1574
04	27.8	12.2	3.5	4.6	1520
08	53.0	23.5	6.8	3.6	1560
12	86.7	36.1	10.4	3.8	1552
20	138	61	17.6	4.2	1546

Table 2: Topographic properties

with ra2D is smaller than with of Abaqus (10hours against 7 days). The power spectrum density of friction noise are shown in Fig. **??**. We remark that the eigenfrequencies of computed noise well match with the peaks of power spectrum density. It means that the coupling between the

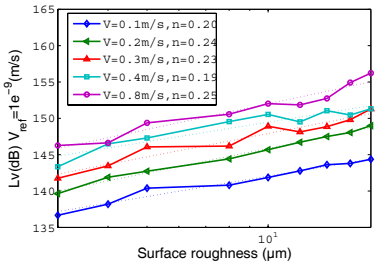

(a) Lv - Rq

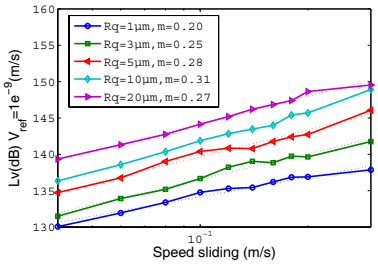

(b) Lv - V

Figure 5: Relation between vibration level and surface roughness, sliding speed

two metal pieces is light. The vibration level Lv(dB) is defined as :

$$\Delta Lv(dB) = 20log(\frac{\Delta V_{RMS}}{V_0}) \quad (12)$$

$$V_{RMS}^2 = \frac{1}{N_{time}} * \frac{1}{N_{node}}\Sigma V_{i,j}^2 \quad (13)$$

Where V0 = 1e-9 m /s is the reference vibrational velocity. VRM is the root mean square of vibrational velocity, $V_{i,j}$ is the velocity of node i at time j. N and Nt are the number of nodes and time steps. The variation of the vibratory level Lv (dB) versus surface roughess and sliding speed is shown in Fig. 5. From these results it is clearly seen that Lv (dB) is simultaneously a linear function of the logarithm of the surface roughness and the slding speed according to the following relationship:

$$\Delta Lv(dB) = 20\log[(\frac{V2}{V1})^m(\frac{Rq2}{Rq1})^n] \quad (14)$$

with $0.19 \leq n \leq 0.25$ and $0.20 \leq m \simeq 0.31$.

7 Conclusion

The system model studied here allows to calculate the local dynamics of two rough surfaces in relative sliding. The equation of motion is solved numerically using the modal developement and double discretization in time and space. Several time integration schemes were programmed and compared. The resulting code, limited to the case plan, is faster than the standard finite element method. The software is validated by comparison with Abaqus, the analytical formula and the experimental results

8 Acknowledgments

Funding support from the Laboratoires d'Excellence (LABEX) and technical support from Federation Lyonnaise

de Modelisation et Sciences Numerique (FLMSN) are acknowledged.

References

[1] Le Bot A., Bou-Chakra E. 2009 Measurement of friction noise versus contact area of rough surfaces weakly loaded. *Tribology Letters.* **vol. 37,** 273-281

[2] Le Bot A., Bou-Chakra E., Michon G. 2011 Dissipation of Vibration in Rough Contact. *Tribology letters* **vol. 41,** 47-53

[3] BAILLET Laurent, SASSI Taoufik 2003 Numerical implementation of different finite element methods for contact problems with friction. *Comptes rendus. M/ ecanique* **vol. 331,** 789-796

[4] Ben Abdelounis H., Le Bot A., Perret-Liaudet J., Zahouani H. 2010 The roughness effect on the frequency of frictional sound. *Wear A.* **vol. 268,** 335-345

[5] OLsson M. 1991 On the fundamental moving load problem. *Jounal of Sound and Vibration* **vol. 145,** 299-307

[6] AKAY Adnan 2002 Acoustics of friction . *The Journal of the Acoustical Society of America* **vol. 111,** 1525-1548

[7] FORD I. J. 1993 roughness effect on friction for multi-asperity contact between surface. *Journal of physics. D, Applied physics* **vol. 26,** 2219-2225

[8] STOIMENOV Boyko L., MARUYAMA Suguru, ADACHI Koshi, KATO Koji 2007 The roughness effect on the frequency of frictional sound. *Tribology international* **vol. 40,** 659-664

[9] A.Meziane, L.Baillet, B.Laulagnet 2010 Experimental and numerical investigation of friction-induced vibration of a beam-on-beam in contact with friction *Applied Acoustics* **vol. 71,** 843-853

[10] G.Dubois, J.Cesbron, H.P.Yin, F.Anfosso-Lédée 2012 International journal of mechanical Sciences *Applied Acoustics* **vol. 54,** 84-94